Proceedings of the ASME 2010 3rd Joint US-European Fluids Engineering Summer Meeting and 8th International Conference on Nanochannels, Microchannels, and Minichannels
FEDSM-ICNMM2010
August 1-5, 2010, Montreal, Canada

FEDSM-ICNMM2010-30364

STUDY THE HEAT TRANSFER PROCESS FROM ELECTRON-PHONON NONEQUILIBRIUM IN THIN GOLD FILM TO GLASS SUBSTRATE THROUGH TRANSIENT THERMOREFLECTANCE MEASUREMENTS

Weigang Ma, Haidong Wang, Xing Zhang*
Key Laboratory for Thermal Science and Power Engineering of Ministry of Education,
Department of Engineering Mechanics, Tsinghua University,
Beijing 100084, People's Republic of China

Wei Wang
National Key Laboratory of Nano/Micro Fabrication Technology,
Institute of Microelectronics, Peking University,
Beijing 100871, People's Republic of China

*Corresponding Author: x-zhang@tsinghua.edu.cn

ABSTRACT

How the energy transfers during electron-phonon nonequilibrium in thin metal films is still an open question, and how to measure the intrinsic thermal transport properties of the material under the covering layer is another challenge. In this paper, the heat transfer process from electron-phonon nonequilibrium in thin gold film to borosilicate glass substrate has been studied by resorting to different segments of the transient thermoreflectance signal, which is obtained from the rear-pump front-probe transient thermoreflectance technique. The gold film, which has a thickness of 23.1 nm, is deposited on the borosilicate glass substrate using using a physical vapor deposition (PVD) approach. Within the framework of the two-temperature model (TTM), the electron-phonon (e-ph) coupling factors of the gold film, which reflect the strength of heat flow from hot electrons to cold phonons, are derived from the signal taken after the first several picoseconds with different pump fluences, and the measured value is $(1.95\text{-}2.05)\times 10^{16}$ W m^{-3} K^{-1}. The electron-phonon coupling factor does not significantly change in response to the pump pulse fluence variation and exhibits little change compared to the bulk gold value 2.4×10^{16} W m^{-3} K^{-1}. Furthermore, the thermal conductivity of the glass substrate is obtained through the thermoreflectance signal between 20 to 140 picoseconds and the value is 3 W m^{-1} K^{-1}.

Keywords: electron-phonon coupling factor, thermal conductivity, gold film, transient thermoreflectance

NOMENCLATURE

t	time (s)
x	spatial coordinate (m)
y	spatial coordinate (m)
S	source term (W m^{-3})
C	heat capacity (J kg^{-1} K^{-1})
G	electron-phonon coupling factor (W m^{-3} K^{-1})
J	laser fluence (W m^{-2})
τ_p	duration of the laser pulse (fs)
δ	optical penetration depth (nm)
R	metal surface reflectance
A	metal absorptance
γ	electron heat capacity constant (J m^{-3} K^{-2})
a	electron temperature dependent coefficient (K^{-1})
b	lattice temperature dependent coefficient (K^{-1})
A_e	electron-electron scattering coefficient (K^{-2} s^{-1})
B_l	electron-phonon scattering coefficient (K^{-1} s^{-1})
v	speed of electrons (m s^{-1})

d	thickness (nm)
D	grain size (nm)
T	temperature (K)
n	electron number density (m^{-3})
K	thermal conductivity (W m^{-1} K^{-1})
Λ	electron mean free path (m)
p	surface scattering parameter, dimensionless
R_g	grain-boundary scattering parameter, dimensionless
α	grain diameter parameter, dimensionless
β	film thickness parameter, dimensionless
k	Boltzmann constant (J K^{-1})
T_D	Debye temperature (K)

Subscripts and superscripts

f	film
b	bulk
e	electron
l	lattice
eq	equilibrium
s	substrate
RT	room temperature
F	Fermi surface

1 INTRODUCTION

Dynamic aspects of the interaction between electrons and phonons in thin metallic film are of great importance not only for the interest of fundamental research but also for broad application, as electron-phonon interactions are of major importance to electrical and thermal transport in metals and govern the formation of the superconducting state [1]. One example is in laser processing, especially laser ablation. Subpicosecond pulses are widely used because of their unique capabilities compared to continuous wave laser and nanosecond pulses: lower ablation threshold [2-5], high precision [6-9], and minimal collateral thermal damage [6, 8]. However, the mechanisms of ultrashort laser ablation are still not thoroughly understood. In the ultrashort laser pulse ablation, the electron and phonon will keep nonequilibrium and the threshold fluence of the laser pulse for melting metal films will be determined by the electron-phonon coupling [10-12]. The other example is to determine the heat transfer pathways from metal to nonmetal across the interface: the electrons of the metal and the phonons of the nonmetal directly couple at the interface, or phonons of metal couple with the electrons in the metal and then couple with the phonons of nonmetal [13].

The nonequilibrium energy exchange between electrons and the lattice was first theoretically evaluated by Kaganov *et al*. [14]. Anisimov *et al.* [15] proposed a phenomenological two-step model to describe the electron temperature and the lattice temperature during short-pulse laser heating of metals. Qiu and Tien [16] derived a more rigorous, two-temperature model from the Boltzmann transport equation. They [17] further studied the size effects on the electron-phonon coupling in thin metallic films and arrived at a conclusion that the electron-phonon coupling will be enhanced due to shortening of the electron mean free path induced by the size reduction. Some experimental studies [18-21] show that the e-ph coupling increases as films become thinner and appear to support the conclusion. However, some experiments [10, 22-28] suggest that the conclusion do not have general validity.

In this paper, the heat transfer process from electron-phonon nonequilibrium in thin gold film to borosilicate glass substrate, B33, has been studied by resorting to different segments of the transient thermoreflectance signal obtained from the transient thermoreflectance measurements. The gold film and B33 glass are selected to be studied for the reason that gold is inoxidizable and B33 glass is transparent. To get rid off the influence of the pump pulse on the thermoreflectance signal, the configuration applied in this paper is rear heating front detection, instead of conventional measurement using front heating front detection type configuration. The measured electron-coupling factor of the thin gold film is $(1.95\text{-}2.05)\times 10^{16}$ W m^{-3} K^{-1}, and does not significantly change in response to the pump pulse fluence variation. Moreover, the e-ph coupling factor of the film exhibits little change compared to the bulk gold value 2.4×10^{16} W m^{-3} K^{-1} [17]. The thermal conductivity of the B33 glass substrate is obtained by studying the thermoreflectance from 20 ps to 140 ps, as the thermal energy is transmitted from thin gold film into the substrate. The measured thermal conductivity is 3 W m^{-1} K^{-1}.

2 EXPERIMENT

A rear-pump front-probe experimental setup, schematically shown in Fig. 1, was employed to monitor the transient thermoreflectance response of the sample after absorption of an ultrashort laser pulse. The ultrashort optical pulses generated from a turnkey Ti:sapphire laser (Spectra Physics, Mai Tai) of wave-length range 800 nm, pulse width 100 fs, and repetition rate 80 MHz, are separated into two orthogonally polarized beams by a polarizing beam splitter (PBS). The intensity ratio can be steplessly adjusted by rotating the half-wave plate. The intense pump beam is modulated by an acousto-optic modulator (AOM) with the frequency of 1 MHz and then focused on the boundary between the gold film and the transparent substrate with a spot diameter of ~100 μm. This creates a transient thermoreflectance occurring at the corresponding frequency that is detected using a lock-in amplifier (LIA). The low power probe beam passes through an optical delay line that is used to increase the optical path length of the probe beam and therefore the time delay with respect to the pump pulse. The probe beam is then focused on the surface opposite to the heated area with a spot diameter of ~50 μm, and used to monitor the heating-induced reflectance change. A Gland prism with an extinction ratio of $\sim10^{-6}$ is placed in front of the detector to filter out the scattered pump light. A lock-in amplifier monitors the detector's response as the probe pulse is delayed in time, resulting in the temporal relaxation profile of the temperature-dependent reflectance of the sample.

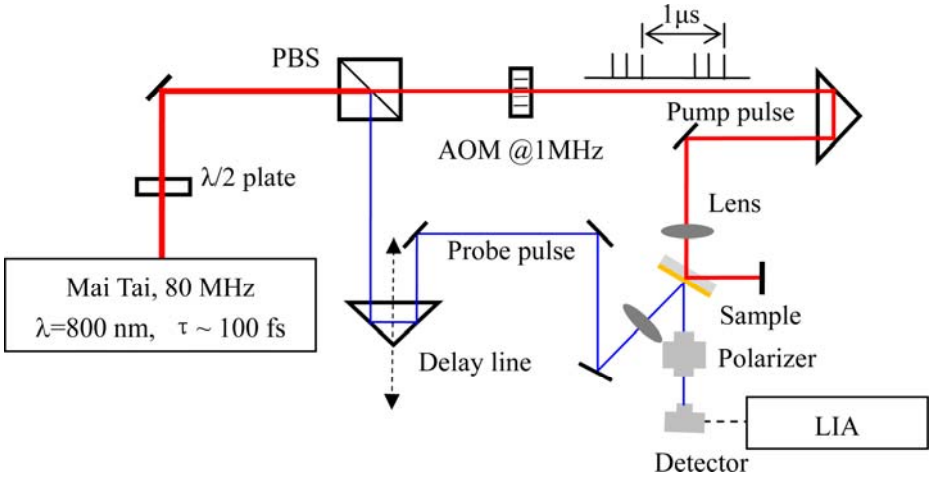

Fig. 1 A SCHEMATIC OF THE KEY ELEMENTS OF THE PUMP-PROBE SYSTEM.

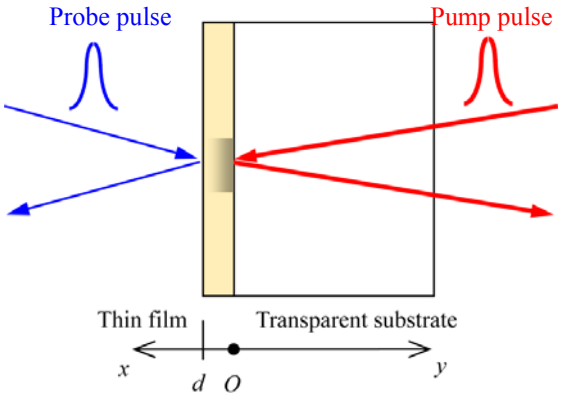

Fig. 2 PHYSICAL MODEL AND COORDINATE SYSTEM [29].

Figure 2 schematically shows the physical model and the coordinate system for the following theoretical analysis. When the sample is excited by the pump pulse, free electrons absorb energy from the laser while the lattice remains cold [15, 16]. On a femtosecond time scale the electrons are thermalized and an electron temperature is established by electron-electron collisions [20]. During the following several picoseconds, the energy transfer from "hot electrons" to the "cold lattice" dominates the energy exchange in gold film and is governed by electron-phonon collisions. The two-temperature model (TTM) [15, 16], assuming that electron distributions and phonon distributions can be characterized in terms of electron temperature T_e and lattice temperature T_l, can be applied to describe the temperature dynamics. It consists of the diffusion equations for the electrons and lattice, coupled by a term proportional to the temperature difference of the two reservoirs multiplied by the electron-phonon coupling factor G, which is used to characterize the strength of the electron-phonon interaction [15, 16, 30],

$$C_e(T_e)\frac{\partial T_e}{\partial t}=\frac{\partial}{\partial x}\left[K(T_e,T_l)\frac{\partial T_e}{\partial x}\right]-G(T_e-T_l)+S(x,t), \quad (1)$$

$$C_l\frac{\partial T_l}{\partial t}=G(T_e-T_l), \quad (2)$$

where $C_e(T_e)$ is the temperature-dependent electronic heat capacity, defined as $C_e=\gamma T_e$ [30], the electron heat capacity constant is taken as 71.4 J m^{-3} K^{-2} [21], $K(T_e, T_l)$ is the effective electron thermal conductivity that accounts for electron-electron and electron-phonon scatterings, defined as $K(T_e, T_l) = K_0[T_e/T_l]$ [30], where K_0 is the equilibrium thermal conductivity 317 W m^{-2} K^{-1} [21]. For a Gaussian laser pulse, the mathematical form of the 1D volumetric laser energy deposited into the film $S(x,t)$ is expressed as [16,30]:

$$S(x,t)=0.94\frac{JA}{\tau_p\delta}\exp\left(-\frac{x}{\delta}-4\ln 2\times\left(\frac{t}{\tau_p}\right)^2\right), \quad (3)$$

where τ_p is the full-width-at-half-maximum (FWHM) duration of the laser pulse. It should be noted that in the present study, the absorptance of the film is carefully measured and the value is 0.08, other than taken as the literature value, 0.06.

Define time t=0 as the moment when the peak of a pump laser pulse arrives at the metal surface, and hence the corresponding initial conditions for both the electron and the lattice systems are [30]:

$$T_e(x,-2\tau_p)=T_l(x,-2\tau_p)=T_0. \quad (4)$$

During the short period of electron-phonon nonequilibrium heat transfer, heat losses from the front and back surfaces of the film can be neglected, leading to the thermal-insulation boundary conditions for both the electron and the lattice systems [30],

$$\left.\frac{\partial T_e}{\partial x}\right|_{x=0}=\left.\frac{\partial T_e}{\partial x}\right|_{x=d}=\left.\frac{\partial T_l}{\partial x}\right|_{x=0}=\left.\frac{\partial T_l}{\partial x}\right|_{x=d}. \quad (5)$$

As stated above, the electron-phonon nonequilibrium heat transfer in thin gold film can be studied by extracting the electron-phonon coupling factor from fitting the TTM predicted temperature profile to the temperature-dependent thermoreflectance response in the initial several picoseconds.

Furthermore, to study the thermal transport as the thermal energy is transmitted from thin gold film into the substrate at a rate proportional to the thermal conductivity of the material, the

difference between the electron and phonon temperatures of the gold film in the initial several picoseconds is negligible. Hence, the thermal transport can be reliably estimated by Fourier's law [31],

$$C_f \frac{\partial T_f}{\partial t} = K_f \frac{\partial^2 T_f}{\partial x^2} + S(x,t), \tag{6}$$

$$C_S \frac{\partial T_S}{\partial t} = K_S \frac{\partial^2 T_S}{\partial y^2}. \tag{7}$$

The initial conditions for both the thin gold film and the substrate can be obtained with the same definition of time t=0 as above,

$$T_f(x,-2\tau_p) = T_s(y,-2\tau_p) = T_0. \tag{8}$$

In the studied period, about one hundred picoseconds, radiation and convection at the air/slab interface can be ignored compared with heat conduction. Considering the interface thermal resistance R_{int}, the temperature-jump and uniform heat flux boundary conditions are imposed at the interface between the thin film and the substrate which is assumed semi-infinite,

$$\left.\frac{\partial T_f}{\partial x}\right|_{x=d} = 0, \tag{9}$$

$$K_f \left.\frac{\partial T_f}{\partial x}\right|_{x=0} = K_s \left.\frac{\partial T_s}{\partial y}\right|_{y=0}, \; T_f(0,t) - T_s(0,t) = -R_{\text{int}} \cdot K_f \left.\frac{\partial T_f}{\partial x}\right|_{x=0}, \tag{10}$$

$$T_s(\infty,t) = T_0. \tag{11}$$

In this way, the heat transfers from the thin gold film into the substrate can be studied. The thermal conductivity of the substrate can be obtained by fitting the temperature profile predicted from the Fourier's law [Eqs. (6) and (7)] to the temperature-dependent thermoreflectance signal.

The electron and phonon temperature changes, resulting from pump pulse heating, can be obtained from reflectivity change detected by the probe pulse. Finally we can get a simplified liner relationship between the reflectance and the electron and phonon temperatures [21, 24, 32]:

$$\Delta R = a\Delta T_e + b\Delta T_l, \tag{12}$$

where the parameters a and b describe how much the temperatures of the electrons and phonons affect the thermoreflectivity. The coefficient a can be extracted from fitting the peak of the electron temperature profile, and the coefficient b is determined by fitting the lattice temperature profile when the electron and phonon systems reach temperature equilibrium again.

3 RESULTS AND DISCUSSION

3.1 Electron-phonon coupling factor

The electron-phonon coupling factor of the thin gold film with thickness of 23.1 nm is measured, which is deposited onto borosilicate glass (B33) using physical vapor deposition (PVD) technique. The borosilicate glass substrate is cleaned by the piranha solution (boiled mixture of sulfuric acid and hydrogen peroxide with volume ratio of 3:1), then washed with deionized water, and dried by nitrogen gas. The thin gold film is deposited on the substrate with a deposition rate of 0.2 nm s^{-1} under vacuum 10^{-4} Pa.

The electron-coupling factor of the film is measured with four different pump fluences (0.96, 0.80, 0.64, 0.48 J m^{-2}) respectively, while the probe fluence is held constant. The transient thermoreflectance response of the film with different pump energy are normalized at the peak reflectance of the maximum energy and shown in Fig. 3 (scatters). On the other hand, the electron and lattice temperatures of the film with different electron and phonon interaction strength are calculated by using the two-temperature model. The time-dependent reflectance changes caused by the electron and lattice temperatures shift are also shown in Fig. 3 (lines). The electron-phonon coupling factor is obtained from optimizing the theoretical prediction to best fit the experimental data.

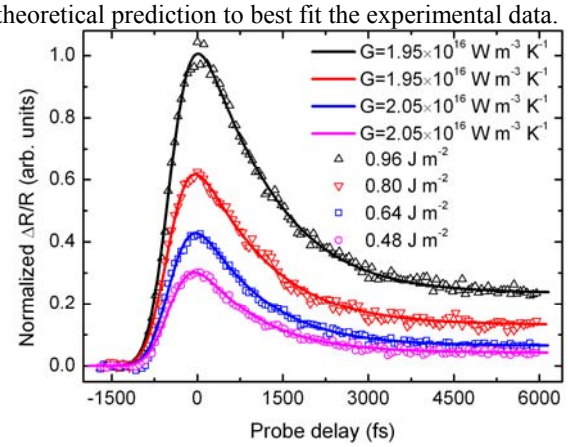

Fig. 3 NORMALIZED TRANSIENT THERMOREFLECTANCE ON 23.1 NM AU/GLASS SAMPLE TAKING WITH DIFFERENT PUMP FULENCES.

From Fig. 3, it can be found that the electron-coupling factor of the thin gold film is (1.95-2.05)×10^{16} W m^{-3} K^{-1} and the measurement uncertainty is ±0.1 W m^{-3} K^{-1}. This agrees well with previous studies, which show that the electron-phonon coupling factor ranges from 2.0 to 3.0×10^{16} W m^{-3} K^{-1} [10, 22-28]. The electron-phonon coupling strength is almost unchanged versus the pump pulse energy within the experimental uncertainty. It appears that this result deviates from the conclusion reached by Chen *et al.* [12] and Hopkins *et al.*[21, 28] which states that the increased electron temperature caused by the higher laser fluence tends to create a subsequent increase in G. However, the maximum electron temperature increment in this study is 67.6 K. Based on the analysis of Chen and co-workers, it can be found that the e-ph coupling factor varies versus the temperature [12],

$$G = G_{RT}\left[\frac{A_e}{B_l}(T_e + T_l) + 1\right], \tag{13}$$

where G_{RT} is the value of e-ph coupling factor when the electron temperature increase tends to zero, the two constants A_e and B_l are functions of the Fermi temperature. For gold, they are A_e=1.2×10^7 K^{-2} s^{-1} and B_l=1.23×10^{11} K^{-1} s^{-1} [33-35]. The ration of the factor G to G_{RT} versus electron temperature increment is shown in Fig. 4.

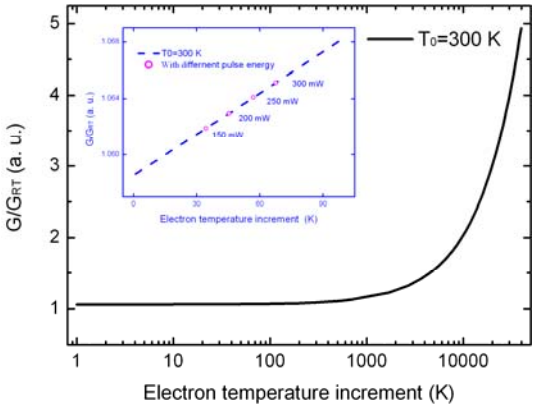

Fig. 4 THE RATIO OF THE ELECTRON-PHONON COUPLING FACTOR VS. ELECTRON TEMPERATURE INCREMENT.

It can be found that the e-ph coupling factor will increase as electron temperature increment increase. However, the temperature-dependent effect is not significant until the temperature increase is on the order of 10^3 K. The e-ph coupling factors change in the studied temperature range are shown in the inset of Fig. 4. We can find that the maximum ratio is 1.065. Such a tiny change will be overwhelmed by the measurement uncertainty. And hence, the measured value of the electron-coupling factor appears not change versus the pump pulse energy.

The thin gold film is investigated via tapping-mode atomic force microscopy (AFM) as shown in Fig. 5, and we can find the film is polycrystalline.

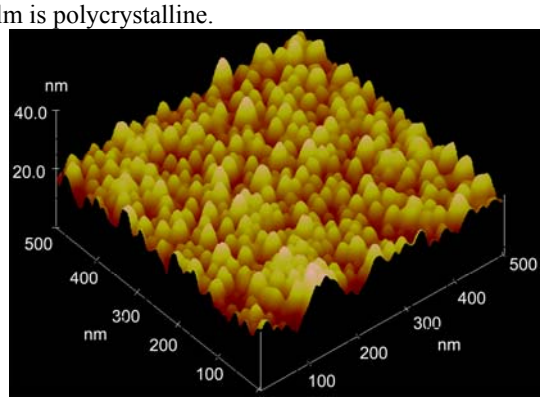

Fig. 5 ATOMIC FORCE MICROSCOPY TAPPING-MODE IMAGE OF THE GOLD FILM.

Qiu and Tien [17] have studied the effect of electron scatterings by film surface and grain boundary on the e-ph coupling based on the fact that these scatterings will shorten the electron mean free path and subsequently increase the electron collision frequency. They developed a simple thermodynamics approach to evaluate G,

$$G=\frac{9}{16}\frac{nk^2T_D^2v_F}{\Lambda(T_l)T_lE_F}, \tag{14}$$

where $\Lambda(T_l)$ is the electron mean free path at the lattice temperature. Finally, they studied the size effects from surface and grain boundary on the G due to the shortening of electron mean free path in thin polycrystalline metallic film,

$$\frac{G_f}{G_b}=\frac{\Lambda_b}{\Lambda_f}=1+\frac{3}{8\beta}(1-p)+\frac{7}{5}\alpha, \tag{15}$$

where $\alpha=\Lambda_bR_g/D(1-R_g)$, $\beta=d/\Lambda_b$, d is the film thickness, D is the mean grain size.

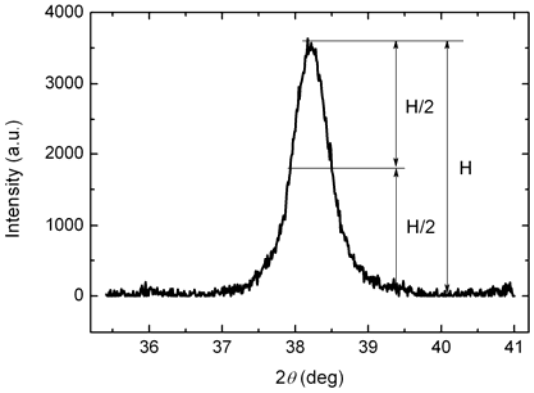

Fig. 6 X-RAY DIFFRACTION SPECTRUM OF GOLD FILM.

The microstructure of the nanofilm has been investigated by x-ray diffraction (XRD) and the diffraction spectrum is presented in Fig. 6. The average size of the crystallites is estimated 15.2 nm from the full width at half maximum (FWHM) of the peaks using the Scherrer equation. For bulk gold, taking the value of each parameter as follows, n=5.9×10^{28} m^{-3}, T_D=165 K, v_F=1.39×10^6 m s^{-1}, E_F=8.82×10^{-19} J [36], and Λ_b(300 K)=37.0 nm, the calculated e-ph coupling factor is G_b=2.4×10^{16} W m^{-3} K^{-1}. The predicted e-ph coupling factors of the film G_f versus the grain boundary reflection coefficient R_g when the surface reflection parameter is taken as p=0 (completely diffuse scattering) and p=1 (completely specular reflexion) are shown in Fig. 7, respectively. From Fig. 7, it can be found that the electron-phonon coupling is nearly the same as that of bulk gold. The predicted value of the film e-ph coupling factor will be within the dashed area. However, it can be found that G_f does not show sharp increase as Qiu and Tien stated.

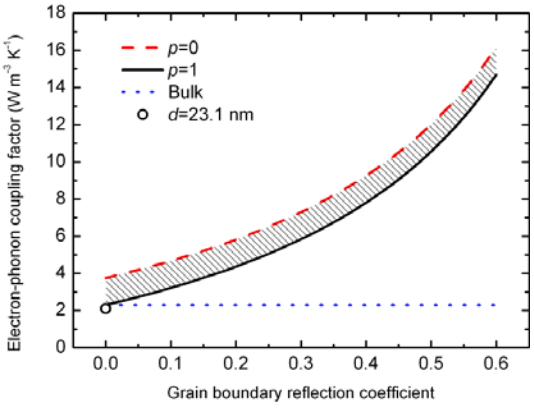

Fig. 7 PREDICTED E-PH COUPLING FACTOR VS. GRAIN BOUNDARY REFLECTION COEFFICIENT.

In order to fit the measured e-ph coupling factor of the film, both the surface reflection parameter and the grain boundary reflection coefficient have to be taken as zero, which may not conform to physical reality. One possible reason is that in thin film, the phonons are softened and the corresponding Debye temperature decreases due to spatial confinement. In the Debye model for phonons, the maximum energy of a phonon is proportional to the Debye temperature [37]. During electron-lattice interactions, electrons gain or lose the energy of a phonon. And hence, the phonon softening in thin film will hinder the electron-phonon coupling. As illustrated by the Qiu-Tien model, the e-ph coupling factor is proportional to the Debye temperature [17]. Now we can find that the size reduction is a double-edged sword in nonequilibrium heat transfer of thin gold film, since it enhances the electron-phonon coupling through shortening the electron mean free path while hinders the coupling through softening the phonons. The overall coupling strength increase or not depend on the relative intensity of the size effects on phonons compared to on electrons. By taking into account the phonon softening in thin film, the present model is expected to explain and predict the change of electron-phonon coupling strength in thin films more reliably.

3.2 Thermal conductivity of the borosilicate glass substrate

As stated above, in order to obtain the e-ph coupling factor, our attention is focused on the initial several picoseconds when electron system and lattice system have their separate temperatures and maintain nonequilibrium. However, the thermal conductivity of the B33 glass is studied in the following time range from 20 ps to 140 ps after the gold film is heated by the pump pulse, as the thermal energy is transmitted from thin gold film into the substrate at a rate proportional to the thermal conductivity of the B33 glass.

The temperature relaxation of the film caused by heat conduction into the substrate is calculated by the Fourier's law [Eqs. (6) and (7)]. As the electron and lattice temperature are the same, and the relationship between the reflectance change and the temperatures of electrons and phonons [Eq. (12)] can be simplified into,

$$\Delta R = c\Delta T_f, \tag{16}$$

where the parameter c, equals to the sum of a and b, can be extracted from fitting the starting point of the studied time range, ie., 20 ps. As shown in Fig. 8, at the initial several picoseconds, the electron temperature decreases rapidly. Subsequently, the electron and phonon remain equilibrium and transfer energy deep into the substrate and the temperature decreases slowly. The thermal conductivity of the B33 glass will determine the temperature relaxation process, and hence it can be obtained by least square fitting the predicted temperature relaxation trace to the measured temporal relaxation profile of the sample temperature-dependent reflectance. The measured value of the thermal conductivity of the substrate is 3 W m^{-1} K^{-1}. For comparison, the predicted temperature relaxation traces when the thermal conductivity is taken as 1 W m^{-1} K^{-1} and 5 W m^{-1} K^{-1} are also shown inset. It can be found that when the thermal conductivity is not taken as 3 W m^{-1} K^{-1}, the predicted relaxation will deviate significantly from the measured trace, which illustrates the substrate thermal conductivity measurement using the present method has a sufficient sensitivity. It should be noted that in the measured signal, there are many fluctuations as shown in Fig. 8, which tends to reduce the measurement advantage. However, it is very difficult to get rid of the fluctuations drastically and subsequently make the signal prefect for the reason that the thermoreflectivity is very small, about 10^{-6}.

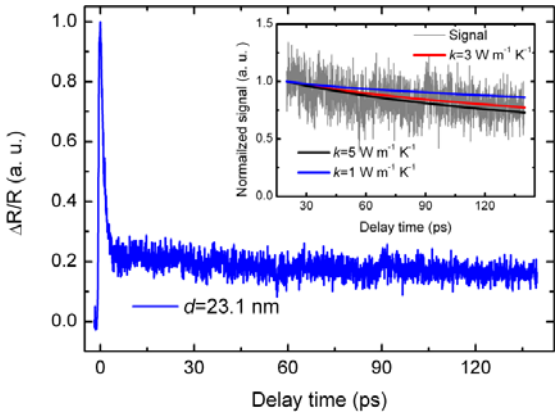

Fig. 8 NORMALIZED TRANSIENT THERMOREFLECTANCE ON 23.1 NM AU/GLASS SAMPLE VS. DELAY TIME.

4 CONCLUSION

The heat transfer process from electron-phonon nonequilibrium in thin gold film to B33 glass substrate has been simultaneously studied by resorting to different segments of the thermoreflectance signal obtained from the rear heating front detection transient thermoreflectance technique. The measured electron-coupling factor of the thin gold film is $(1.95\text{-}2.05)\times10^{16}$ W m^{-3} K^{-1}, does not significantly change in response to the pump pulse fluence variation. From analysis, it can be found that the electron temperature increment is not large enough and therefore only leads to a tiny e-ph coupling factor change, which will be overwhelmed by the measurement uncertainty. Moreover, the e-ph coupling factor of the film exhibits little change compared to the bulk gold value 2.4×10^{16} W m^{-3} K^{-1}, which shows that the size reduction of the thin film is a double-edged sword in nonequilibrium heat transfer, since it enhances the electron-phonon coupling through shortening the electrons mean free path while hinders the coupling through softening the phonons. The thermal conductivity of the B33 glass substrate is obtained by studying the transient thermoreflectance from 20 ps to 140 ps as the thermal energy is transmitted from thin gold film into the substrate. The measured thermal conductivity is 3 W m^{-1} K^{-1}.

ACKNOWLEDGMENTS

This work was supported by the National Natural Science Foundation of China (Grant Nos 50730006 and 50976053).

REFERENCES

[1] R. H. M. Groeneveld, R. Sprik and A. Lagendijk, 1995, Femtosecond Spectroscopy of Electron-Electron and Electron-Phonon Energy Relaxation in Ag and Au, Phys. Rev. B, 51(17), pp.11433-11445.

[2] S. Preuss, A. Demchuk and M. Stuke, 1995, Subpicosecond UV Laser-Ablation of Metals, Appl. Phys. A-Mater. Sci. Process., 61(1), pp.33-37.

[3] B. C. Stuart, M. D. Feit, S. Herman, A. M. Rubenchik, B. W. Shore and M. D. Perry, 1996, Optical Ablation by High-Power Short-Pulse Lasers, J. Opt. Soc. Am. B-Opt. Phys., 13(2), pp.459-468.

[4] J. Güdde, J. Hohlfeld, J. G. Müller and E. Matthias, 1998, Damage Threshold Dependence on Electron-Phonon Coupling in Au and Ni Films, Appl. Surf. Sci., 127-129, pp.40-45.

[5] A. Semerok, C. Chaleard, V. Detalle, J. L. Lacour, P. Mauchien, P. Meynadier, C. Nouvellon, B. Salle, P. Palianov, M. Perdrix and G. Petite, 1999, Experimental Investigations of Laser Ablation Efficiency of Pure Metals with Femto, Pico and Nanosecond Pulses, Appl. Surf. Sci., 138, pp.311-314.

[6] C. Momma, B. N. Chichkov, S. Nolte, F. vonAlvensleben, A. Tunnermann, H. Welling and B. Wellegehausen, 1996, Short-Pulse Laser Ablation of Solid Targets, Opt. Commun., 129(1-2), pp.134-142.

[7] S. Nolte, C. Momma, H. Jacobs, A. Tunnermann, B. N. Chichkov, B. Wellegehausen and H. Welling, 1997, Ablation of Metals by Ultrashort Laser Pulses, J. Opt. Soc. Am. B-Opt. Phys., 14(7), pp.2716-2722.

[8] M. D. Shirk and P. A. Molian, 1998, A Review of Ultrashort Pulsed Laser Ablation of Materials, Journal of Laser Applications, 10(1), pp.18-28.

[9] M. Lenzner, J. Kruger, W. Kautek and F. Krausz, 1999, Precision Laser Ablation of Dielectrics in the 10-Fs Regime, Appl. Phys. A-Mater. Sci. Process., 68(3), pp.369-371.

[10] S. S. Wellershoff, J. Hohlfeld, J. Gudde and E. Matthias, 1999, The Role of Electron-Phonon Coupling in Femtosecond Laser Damage of Metals, Appl. Phys. A-Mater. Sci. Process., 69, pp.S99-S107.

[11] J. K. Chen and J. E. Beraun, 2003, Modelling of Ultrashort Laser Ablation of Gold Films in Vacuum, J. Opt. A-Pure Appl. Opt., 5(3), pp.168-173.

[12] J. K. Chen, W. P. Latham and J. E. Beraun, 2005, The Role of Electron-Phonon Coupling in Ultrafast Laser Heating, Journal of Laser Applications, 17(1), pp.63-68.

[13] A. Majumdar and P. Reddy, 2004, Role of Electron-Phonon Coupling in Thermal Conductance of Metal-Nonmetal Interfaces, Appl. Phys. Lett., 84(23), pp.4768-4770.

[14] M. Kaganov, I. Lifshitz and L. Tanatarov, 1957, Relaxation between Electrons and Crystalline Lattices, Soviet Physics-JETP, 4, pp.173-178.

[15] S. Anisimov, B. Kapeliovich and T. Perelman, 1974, Electron Emission from Metal Surfaces Exposed to Ultrashort Laser Pulses, Soviet Physics-JETP, 39, pp.375-377.

[16] T. Q. Qiu and C. L. Tien, 1993, Heat-Transfer Mechanisms During Short-Pulse Laser-Heating of Metals, J. Heat Transf.-Trans. ASME, 115(4), pp.835-841.

[17] T. Q. Qiu and C. L. Tien, 1993, Size Effects on Nonequilibrium Laser-Heating of Metal-Films, J. Heat Transf.-Trans. ASME, 115(4), pp.842-847.

[18] H. E. Elsayed-Ali, T. Juhasz, G. O. Smith and W. E. Bron, 1991, Femtosecond Thermoreflectivity and Thermotransmissivity of Polycrystalline and Single-Crystalline Gold-Films, Phys. Rev. B, 43(5), pp.4488-4491.

[19] T. Juhasz, H. E. Elsayedali, G. O. Smith, C. Suarez and W. E. Bron, 1993, Direct Measurements of the Transport of Nonequilibrium Electrons in Gold-Films with Different Crystal-Structures, Phys. Rev. B, 48(20), pp.15488-15491.

[20] J. L. Hostetler, A. N. Smith, D. M. Czajkowsky and P. M. Norris, 1999, Measurement of the Electron-Phonon Coupling Factor Dependence on Film Thickness and Grain Size in Au, Cr, and Al, Appl. Optics, 38(16), pp.3614-3620.

[21] P. E. Hopkins, J. L. Kassebaum and P. M. Norris, 2009, Effects of Electron Scattering at Metal-Nonmetal Interfaces on Electron-Phonon Equilibration in Gold Films, J. Appl. Phys., 105(2), 023710.

[22] R. W. Schoenlein, W. Z. Lin, J. G. Fujimoto and G. L. Eesley, 1987, Femtosecond Studies of Nonequilibrium Electronic Processes in Metals, Phys. Rev. Lett., 58(16), pp.1680-1683.

[23] P. B. Allen, 1987, Theory of Thermal Relaxation of Electrons in Metals, Phys. Rev. Lett., 59(13), pp.1460-1463.

[24] S. D. Brorson, A. Kazeroonian, J. S. Moodera, D. W. Face, T. K. Cheng, E. P. Ippen, M. S. Dresselhaus and G. Dresselhaus, 1990, Femtosecond Room-Temperature Measurement of the Electron-Phonon Coupling Constant-Lambda in Metallic Superconductors, Phys. Rev. Lett., 64(18), pp.2172-2175.

[25] C. K. Sun, F. Vallee, L. H. Acioli, E. P. Ippen and J. G. Fujimoto, 1994, Femtosecond-Tunable Measurement of Electron Thermalization in Gold, Phys. Rev. B, 50(20), pp.15337-15348.

[26] J. Hohlfeld, S. S. Wellershoff, J. Gudde, U. Conrad, V. Jahnke and E. Matthias, 2000, Electron and Lattice Dynamics Following Optical Excitation of Metals, Chem. Phys., 251(1-3), pp.237-258.

[27] A. N. Smith and P. M. Norris, 2001, Influence of Intraband Transitions on the Electron Thermoreflectance Response of Metals, Appl. Phys. Lett., 78(9), pp.1240-1242.
[28] P. E. Hopkins and P. M. Norris, 2007, Substrate Influence in Electron-Phonon Coupling Measurements in Thin Au Films, Applied Surface Science, 253(15), pp.6289-6294.
[29] N. Taketoshi, T. Baba and A. Ono, 2001, Development of a Thermal Diffusivity Measurement System for Metal Thin Films Using a Picosecond Thermoreflectance Technique, Meas. Sci. Technol., 12(12), pp.2064-2073.
[30] T. Q. Qiu and C. L. Tien, 1994, Femtosecond Laser-Heating of Multilayer Metals .1. Analysis, Int. J. Heat Mass Transf., 37(17), pp.2789-2797.
[31] R. J. Stevens, A. N. Smith and P. M. Norris, 2005, Measurement of Thermal Boundary Conductance of a Series of Metal-Dielectric Interfaces by the Transient Thermoreflectance Technique, J. Heat Transf.-Trans. ASME, 127(3), pp.315-322.
[32] P. M. Norris, A. P. Caffrey, R. J. Stevens, J. M. Klopf, J. T. McLeskey and A. N. Smith, 2003, Femtosecond Pump-Probe Nondestructive Examination of Materials (Invited), Rev. Sci. Instrum., 74(1), pp.400-406.
[33] A. H. Macdonald, 1980, Electron-Phonon Enhancement of Electron-Electron Scattering in A1, Phys. Rev. Lett., 44(7), pp.489-493.
[34] D. E. Gray, 1972, American Institute of Physics Handbook, 3rd Ed., Mcgrawhill, New York.
[35] X. Y. Wang, D. M. Riffe, Y. S. Lee and M. C. Downer, 1994, Time-Resolved Electron-Temperature Measurement in a Highly Excited Gold Target Using Femtosecond Thermionic Emission, Phys. Rev. B, 50(11), pp.8016-8019.
[36] C. Kittel, 1976, Introduction to Solid State Physics, 5th Ed., Wiley, New York.
[37] J. M. Ziman, 2001, Electrons and Phonons, Oxford University Press, Oxford.